Calculating $np\ ^1S_0$ scattering phase shifts using the Lippmann-Schwinger equation and the variable phase approach

Brandon Elman, Brenden Longfellow, and Daniel Votaw
(Dated: November 24, 2017)

We present results of solving the Lippmann-Schwinger equation for a neutron-proton system, and relate the $np\ ^1S_0$ phase shifts obtained to those extracted from the experimental cross sections compiled by the Nijmegen group [1]. We benchmark our code using the known phase shifts from a square well potential, and then verify our results for the potential using the variable phase approach.

I. INTRODUCTION

A. Lippmann-Schwinger Equation

The concept of scattering phase shifts serves as a useful connection between theories of nucleon-nucleon (NN) interactions and experimental data. With some given form of the NN interaction, one just has to solve the time-independent Schrödinger equation (TISE) [Eq. 1] to obtain the scattering wavefunctions, to which asymptotic boundary conditions can be applied to extract S-matrix elements and phase shifts.

$$\hat{H}|\Psi\rangle = E|\Psi\rangle \tag{1}$$

It will be assumed that the Hamiltonian for the system can be written as a free Hamiltonian plus a perturbative, central interaction term [Eqs. 2].

$$\hat{H} = \hat{H}_0 + \hat{V},\ [\hat{H}, \hat{L}_z] = [\hat{H}, \vec{L}^2] = 0 \tag{2}$$

The TISE can be cast into a form which can be expanded in a perturbation series, and is more amenable to numerical methods, called the Lippmann-Schwinger equation [Eq. 3].

$$|\Psi\rangle = |\phi\rangle + \hat{G}(E)\hat{V}|\Psi\rangle \tag{3}$$

This equation allows for the iterative calculation of the wavefunction (Ψ) given an eigenstate of the free Hamiltonian (ϕ), the interaction potential ($\hat{V}$), and a Green's function operator ($\hat{G}$). Exploiting the rotational symmetry of the Hamiltonian, this equation can be expanded in terms of partial waves, and once projected onto the momentum basis, it becomes an integral equation which can be solved numerically for a given partial wave.

The asymptotic form of the s-wave scattering wavefunction should have a dependence given by Eq. 4.

$$\langle \vec{r}|\Psi^{sc}_{\ell=0}\rangle \overset{r\to\infty}{\propto} \frac{\sin\big(kr + \delta_0\big)}{r} \tag{4}$$

The goal then is to extract the s-wave phase shift (δ_0) from the solution of the integral form of the Lippmann-Schwinger equation. The results of the calculation can be compared to experimental NN scattering data, compiled in the Nijmegen database, to test the validity of a model for the NN interaction potential.

μ	V_1	V_2	V_3	c_1	c_2	c_3
$0.7fm^{-1}$	-10.463 MeV	-1650.6 MeV	6484.3 MeV	1	4	7

TABLE I. Parameters used for our nucleon-nucleon potential

The potential that was used in this work is given by Eq. 5, and the parameters are given in Table 1.

$$V(r) = \sum_{i=1}^{3} V_i \frac{\exp\big(-c_i\mu r\big)}{\mu r} \tag{5}$$

The Lippmann-Schwinger equation can be rewritten in terms of the R-matrix ($R_\ell(k,k')$) and the momentum-space form of the potential given in Eq. 5 for a given partial wave ($V_\ell(k,k')$), and the result is shown in Eq. 6.

$$R_\ell(k,k') = V_\ell(k,k') + \frac{2}{\pi}\hat{P}\int_0^\infty V_\ell(k,q)\frac{q^2dq}{E - q^2/m}R_\ell(q,k') \tag{6}$$

And finally, the s-wave phase shift can be extracted from the on-shell R-matrix element for the incoming momentum k_0 [Eq. 7].

$$\delta_0 = \arctan\big(-mk_0R_0(k_0,k_0)\big) \tag{7}$$

This calculated phase shift is the quantity which will be directly compared to data from the Nijmegen database in order to evaluate the validity of this choice of NN potential.

To ensure that the method is being applied correctly, it will be checked for a test case where the phase shift can be calculated analytically. The simplest such case would be a finite spherical well with $V(r) = -V_0\Theta(R-r)$.

B. Variable Phase Approach

An alternate method for calculating scattering phase shifts is the variable phase approach (VPA). Consider the $l = 0$ partial wave for a local potential $V(r)$. The

truncated potential $V_\rho(r)$ [Eq. 8] is the potential for $r \leq \rho$ and zero for $r > \rho$.

$$V_\rho(r) = V(r)\Theta(\rho - r) \tag{8}$$

The phase shift for the truncated potential at momentum k, $\delta(k,\rho)$, is equal to the phase shift for the full potential in the limit of large ρ. Following Calogero [2], the differential equation for $\delta(k,r)$ at fixed k for $l = 0$ is given by Eq. 9.

$$\frac{d\delta(k,r)}{dr} = \frac{-2M}{\hbar^2 k} V(r) \sin^2[kr + \delta(k,r)] \tag{9}$$

In Eq. 9, M is the reduced mass of the system (NN in this case) and the initial condition for the differential equation is $\delta(k,0) = 0$. It can be seen from Eq. 9 that a fully attractive potential gives a positive phase shift and a fully repulsive potential gives a negative phase shift since $\sin^2 x$, M, and k are positive. If $V(r)$ is negative (attractive potential) then $\frac{d\delta(k,r)}{dr}$ is positive and since $\delta(k,0) = 0$, the accumulated phase shift with r will be positive.

The VPA builds in Levinson's theorem, which relates the number of bound states n with the phase shift at zero energy by $\delta(0) = n\pi$, since the condition that the phase shift for large energy goes to zero ($\delta(k \to \infty) = 0$) is met. This can be seen from the $1/k$ factor in Eq. 9. Integrating both sides of Eq. 9 from $r = 0$ to ∞ gives $\delta(k) \sim 1/k \int_0^\infty V(r) \sin^2[kr + \delta(k,r)]dr$. For potentials of the Yukawa form, the integral is finite since the $\sin^2[kr + \delta(k,r)]$ term is zero for $r = 0$ (and wins out when using L'Hospital's rule). Since $\sin^2 x \leq 1$, the integral for $r > 0$ will be less than or equal to the integral of the potential. Therefore, $\delta(k)$ will be proportional to $1/k$ and go to zero for large energy, as desired.

The VPA was implemented by simply numerically solving the differential equation using Mathematica.

II. METHODS

The method used to solve the implicit integral form of the Lippmann-Schwinger equation was Gaussian quadrature integration using Legendre polynomials. For convenience, the equation is solved in momentum space, so momentum space is discretized into an $N \times N$ mesh of lattice points. Definite integrals are approximated as discrete sums of the form $\int_a^b f(x)\, dx \approx \sum_{i=1}^N w_i f(x_i)$. A mapping must then be used between the typical domain of the Legendre polynomials ($x_i \in [-1,1]$) and the radial coordinate in momentum space ($k_i \in [0,\infty)$). The mapping for the integration mesh points is given by Eq. 8, and the analogous mapping for the integration weights is given in Eq. 9.

$$k_i = \hbar c \tan\left(\frac{\pi}{4}(1 + x_i)\right) \tag{10}$$

$$\omega_i = \hbar c \frac{\pi}{4} \frac{w_i}{\cos^2\left(\frac{\pi}{4}(1 + x_i)\right)} \tag{11}$$

The discretized version of Eq. 6, with the Cauchy principal value operator removed, is given by Eq. 10.

$$R(k,k') = V(k,k') + \frac{2m}{\pi} \sum_{j=1}^N \frac{\omega_j k_j^2 V(k,k_j) R(K_j,k')}{k_0^2 - k_j^2} - \frac{2m}{\pi} \sum_{n=1}^N \frac{\omega_n}{k_0^2 - k_n^2} \tag{12}$$

Finally, the equation which we solve for the R-matrix elements takes the form of Eq. 11.

$$R = A^{-1} V \tag{13}$$

Where the matrix A is defined by Eq. 12.

$$A_{ij} = \delta_{ij} - \frac{2m}{\pi} V(k_i,k_j) \frac{\omega_j k_j^2}{k_0^2 - k_j^2} \tag{14}$$

III. RESULTS

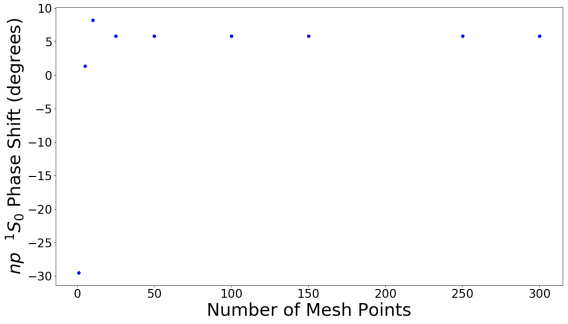

FIG. 1. Convergence results for $E_{lab} = 200$ MeV. Results clearly converge when more than 50 mesh points are used.

First, it was necessary to determine a proper number of mesh points to ensure the convergence of our results. The calculated phase shift as a function of number of mesh points is shown in Figure 1. Note that the calculation clearly converges when more than 50 mesh points are used. Therefore, we chose approximately 100 mesh points for each shown calculated phase shift. Because we must only use mesh points for which $k \neq k_0$, each calculation used either 101 or 102 mesh points, depending on whether the chosen k_0 was close to any value of k in the mesh.

Both our matrix inversion calculation and our VPA calculation completely reproduced the analytically determined phase shifts for a square well potential, as shown

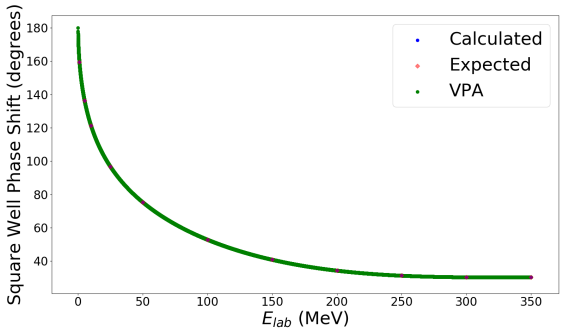

FIG. 2. There is almost exact agreement between analytical results for the phase shift using a square well potential (red diamonds) with both calculated results (blue circles) and results from the VPA calculation (green circles).

in Figure 2. The square well was chosen to have depth of 50 MeV and a cutoff radius of 1.97 fm. This benchmark shows that the calculation is able to reproduce the results for a simple test case. We can now calculate the real np $^1S_0$ phase shift and compare to experiment.

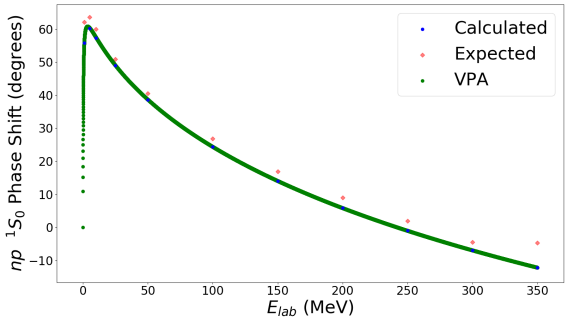

FIG. 3. There is a consistent underestimation for calculated results (blue circles) compared to results from experiment as determined by Nijmegen group (red diamonds) [1], but the VPA method is consistent with the calculated results.

Our results for the comparison with the experimentally determined phase shift by the Nijmegen group and results from the variable phase analysis is shown in Figure 3. The phase shift is consistently underestimated in comparison with the experimental result; however, the shape is well reproduced by the calculation. The results from the variable phase approach are entirely consistent with the calculated results.

From Levinsons's theorem and the VPA results in Fig. 3, we can see that the NN potential given by Eq. 5 with parameters from Table I does not support a bound state for scattering in the $^1S_0$ channel since $\delta(0) = 0$. By adjusting the strength of the longest ranged component of this potential to about $V_1 = -14.7$ MeV, $\delta(0) = \pi$ and there is one bound state.

One should note that there is not a unique potential insofar as low-energy data is concerned. The effective range expansion for low k and $l = 0$ is given by

$$k \cot \delta_0(k) = \frac{-1}{a_0} + \frac{1}{2} r_o k^2 + ... \tag{15}$$

Using the NN potential of Eq. 5 at $k = 0.01$ fm^{-1} and 0.02 fm^{-1}, values of a_0 = -17.6442 fm and $r_0 = 2.77358$ fm are extracted. Using a finite spherical well cut off at 2.6193 fm with depth 13.2791 MeV gives nearly identical values for a_0 and r_0.

IV. CONCLUSIONS

We were able to reproduce the phase shifts for the square well potential test case and the experimentally determined phase shifts for np $^1S_0$ from the Nijmegen group using the Lippmann-Schwinger equation and the VPA. One possible extension to this project could be the inclusion of more realistic nuclear forces. It would be interesting to understand why the potential we used, which was simply the sum of a few Yukawa-like terms, was able to reproduce the shape of the phase shifts so well. Furthermore, another interesting aspect to explore would be what is missing from the simple potential description that results in the slight underestimation of the phase shift in both the calculation and the variable phase analysis.

Note that more details are provided in the submitted C++ code for numerically solving the Lippman-Schwinger equation in momentum space and the submitted Mathematica code for calculating scattering phase shifts using the variable phase approach.

[1] V. G. J. Stoks, R. A. M. Klomp, M. C. M. Rentmeester, and J. J. de Swart, Phys. Rev. C **48**, 792 (1993).

[2] F. Calogero, *The Variable Phase Approach to Potential Scattering* (Academic Press, New York, 1967).